Kinetic Parameters of Petroleum Coke Gasification for Modelling Chemical-Looping Combustion Systems

Agnieszka Korus, Adam Klimanek, Slawomir Sladek, Andrzej Szlęk, Airy Tilland, Stéphane Bertholin, Nils Erland L. Haugen

Kinetic parameters of petroleum coke gasification for modelling chemical-looping combustion systems

Agnieszka Korus[a,1], Adam Klimanek[a], Sławomir Sładek[a], Andrzej Szlęk[a], Airy Tilland[b], Stéphane Bertholin[b], Nils Erland L. Haugen[c]

[a] Department of Thermal Technology, Silesian University of Technology, Gliwice, Poland

[b] IFP Energies nouvelles, BP3, 69360 Solaize, France

[c] SINTEF Energy Research, Trondheim N-7465, Norway

Abstract

One of the best low-cost approaches for capturing carbon dioxide from the combustion of solid fuels is chemical looping combustion (CLC) technology, where the processes of fuel oxidation and extraction of oxygen from the air are split in two separate reactors. In order to model the petroleum coke (petcoke) conversion in a CLC method, detailed knowledge about the reactions of pet-coke with O_2, CO_2, and H_2O at temperatures between 750 and 1100 □ is required. Due to the lack of sufficient literature data, in this paper, the reactivity of these reactions is investigated in a custom-built test rig that enabled measurements of the mass loss of the fuel sample and the composition of the released gases. The Avrami, Random Pore, Shrinking Core, and Hybrid models were applied to the experimental results to determine the kinetic parameters of petcoke gasification. At temperatures up to 1000 □, the reaction with CO_2 was found to be negligibly slow. An activation energy of 103.91 kJ/mol was obtained for

[1] Corresponding author, E-mail: agnieszka.korus@polsl.pl (Agnieszka Korus)

petcoke gasification in 10 – 40 vol.% of H_2O, while a value of 15.87 kJ/mol was found for oxidation in 2 – 4 vol.% O_2, as described by best-fitting models, i.e. Hybrid and Random Pore models, respectively.

Keywords:

Petroleum coke; gasification; chemical-looping combustion

1. Introduction

The production of petroleum coke (petcoke), a by-product of the oil refining process, is constantly increasing due to the high demand for oil-derived fuels and chemicals [1]. This highly calorific material can, therefore, be acquired in abundance at a low cost to produce energy or gaseous fuels [2]. The advantage of using petcoke as a feedstock for thermochemical conversion processes is its high heating value, approximately 20 % higher than that of coal, and its low ash content (0.1 – 0.3 %) [3].

Due to the need to incorporate carbon capture and sequestration (CCS) into the thermochemical conversion of carbonaceous fuels, chemical looping combustion (CLC) technology has become an attractive alternative to conventional combustion methods. The main reason for this is that the use of oxygen carriers that are transported between the air and the fuel reactors essentially results in an oxy-fuel process without the energy penalty associated with the cryogenic oxygen separation process of a regular oxy-fuel process. Although CLC was initially designated for gaseous fuel utilisation, the conversion of solids is also feasible, but it requires a gasifying agent, e.g. H_2O or CO_2, to act as the gaseous intermediate between the solids – oxygen carrier and fuel [4,5]. The feasibility studies on

large-scale CLC installations have confirmed the low cost of the CO_2 capture integration [5], thus increasing the importance of developing this technology to achieve zero or even negative greenhouse gas emissions. To optimise the CLC reactor design, the detailed kinetic data on solid fuel gasification under the conditions characteristic for this technology must be acquired. Therefore, the purpose of this paper is to obtain accurate kinetic parameters for petcoke gasification through kinetic modelling of experimental data.

No clear correlation between the main physicochemical properties of the petcoke and its conversion rate have been established thus far. The parameters such as the specific surface area or volatile matter content do not vary significantly between various samples and they are not responsible for the different kinetics of petcoke oxidation [6]. However, the metals content in petroleum coke can be relatively diverse and these elements can have a non-negligible, yet difficult to quantify, catalytic effect on the petcoke conversion [6,7]. Among others, vanadium, iron, or alkali and alkaline earth metals have been reported to have a significant impact on petcoke gasification and combustion kinetics [6,8,9].

The focus of this study is low-sulphur Chinese petcoke selected for testing at the 3MW CLC reactor designed in the scope of the CHEERS project[2]. Even though some studies of petcoke thermochemical reactivity already exist in the literature [3,8–11], the reactivity of this particular petcoke has not previously been studied. Even more importantly, the kinetic data for CLC conditions, which require high temperatures and low oxygen concentrations, do not exist. Thus, an examination of the thermochemical conversion of the actual material selected for the pilot CLC reactor development, including the exact particle size range and gasification agent concentration, was required to provide accurate data on the apparent kinetic parameters to successfully model the reactor operation. The existing work on petcoke reactions with

[2] CHEERS is jointly funded by the European Union's Horizon 2020 Research and Innovation Program (764697) and the Chinese Ministry of Science and Technology (MOST). See http://cheers-clc.eu/ for more information.

oxygen typically focuses on combustion, thus the experiments are carried out at lower temperatures (400 – 600 □) and higher concentrations of oxidiser (>20 vol.%) [7,12] than the experiments performed in this work. E.g., Gajera et al. [13] examined petcoke conversion in pure O_2 flow at temperatures up to 900 C. Gasification tests are also usually performed with undiluted oxidising agent, such as petcoke conversion in TGA in a pure flow of steam performed by Edreis et al. [14]. Some petcoke gasification tests carried out at temperatures above 1000 ℃ can be found in recently published works [15–19]. However, these reports are often oriented on the fundamental research on the petcoke kinetics, thus comprising thermogravimetric experiments with small sample sizes and the reaction atmosphere limited to pure CO_2. E.g., Wei et al. [17,20] examined the effects of the addition of biomass leachates and Yu et al. [15] the addition of biomass ash on the petcoke gasification. Meanwhile, the conditions for gasification in a CLC reactor require presence of steam or oxygen. It is also beneficial to conduct the application-oriented research in a larger scale than the instrumental analysis such as TGA. Lulu et al. [21] examined petcoke gasification with O_2 and H_2O at 900 ℃ in a fluidized bed, which represented a CLC reactor, using large sample of 0.75 g. Wei et al. [19] used a horizontal furnace with a 50 mg petcoke sample placed in a quartz boat crucible to examine CO_2 gasification at temperatures up to 1200 ℃, while Wang et al. [22] carried out steam gasification tests at 650 – 750 ℃ with 20 g sample in a fixed bed reactor. Liu et al. [23] conducted tests in a 30 kW chemical looping combustion unit. However, the experiments carried out in the larger facilities focused mainly on the operational aspects of these reactors, i.e. monitoring the conversion efficiency or the evolved gases composition, etc., and they do not provide any kinetic data. Zhang et al. [24] presented a robust model of petcoke conversion in 15 – 50 vol.% of steam and 0 – 3 vol.% oxygen based on the experiments in the entrained flow gasifier with a 60 g/h carbon feeding rate. The combined array design methodology allowed for an accurate description of the process, however, these

results cannot be directly incorporated into the deterministic models for petcoke conversion. Although the existing research on petcoke conversion is extensive, there is a lack of kinetic parameters determined at the conditions relevant for gasification in chemical looping combustion units, i.e. based on the experimental work performed in the larger reactor, thus comprising more representative samples, and carried out in the oxidising agent concentrations up to 40 vol.% at the temperatures up to 1000 ℃.

To provide relevant data for the CHEERS project, measurements were conducted in a custom-built test rig that allowed the use of a wider size fraction and higher sample mass than thermogravimetric (TGA) experiments, which typically focus on samples with narrow particles size ranges and lower sample masses <10 mg [8,11,25–27]. The unique construction of the test rig, which has a crucible with a fritted bottom, enables the gas flow through the sample. Improved sample penetration by the oxidising gases reduces the diffusional resistance at high temperatures. Therefore, the kinetic parameters for the conversion not affected by the external diffusion could be obtained for the temperatures as high as 950 □. The design also allows the use of a larger, more representative, sample size than conventional TGA, and the particle size range wide enough to represent the heterogenous fraction of fuel particles used in the industrial scale applications. Moreover, gasification tests for CO_2 partial pressures <0.1 MPa and steam/CO_2 mixtures were performed to meet the conditions relevant for chemical looping gasification, as opposed to the typical kinetic experiments carried out in atmospheres with a single gasifying agent [8–11,25,26]. The combination of the mass loss measurements and analysis of the gases evolved during gasification in CO_2, H_2O, CO_2/H_2O and O_2 provide insight into the nature of petcoke conversion. Finally, the kinetic parameters are fitted using the Avrami, Random Pore, Shrinking Core, and Hybrid Model, and the most suitable approximations are identified for each gasification agent. These most common and universal models were chosen to ensure that the obtained kinetics could be easily applied to the global

models of the entire gasification installations, e.g. CLC-CCS systems. E.g., the Random Pore Model and the Shrinking Core Model were successfully used to describe thermochemical conversion of petcoke in numerous thermogravimetric experiments [14,16,18,20,28]. The experimental work and following calculations provided the apparent kinetics of petcoke conversion under the conditions and for the particle sizes typical for chemical looping gasification, which is necessary for the design and modelling of the pilot installation yet has not been addressed in the previously published works.

2. Experimental

2.1. Materials

The petroleum coke (petcoke) used for the kinetic studies was a low-sulphur Chinese petcoke, which was also used as the main fuel in the CHEERS project. The reported raw petcoke composition on dry basis is: C – 91.2, H – 4.13, O – 1.44, N – 2.52, and S – 0.51 wt.% and ash 0.2 wt.% (by diff.).

Particles in the size range 100 – 300 µm were used in the experiments. Some preliminary tests with a larger fraction (300 – 500 µm) were also carried out (as presented in the Supplement S1); although the results were similar at lower temperatures and oxidiser concentrations, under the more reactive atmospheres (e.g. 40 vol.% H_2O at 1000 □) the gasification time increased by 25 % when the larger fraction was used. This means that the internal diffusion within the petcoke particles plays a nonnegligible role during conversion under more reactive conditions (high temperatures and oxidiser concentrations). The influence of the external diffusion was limited due to the construction of the test rig (a porous crucible that allows for an unrestrained gas flow through the sample bed) and limitation of the analysis to the temperatures characteristic for the kinetic regime. Thus, the obtained parameters represent the

apparent kinetics, which include only internal diffusion, and they are relevant for the examined particle size that was chosen to best represent the fuel used in the CLC unit. Therefore, for the successful utilisation of these results for other applications, external diffusion resistance should be incorporated into the presented model, adequately to the conditions in the given reactor.

To avoid contaminating the test rig with released tars, the petcoke was devolatilised prior to the experiments. The material was heated to 600 □ in a N_2 flow with a 10 □/min heating rate followed by a 30 min isotherm. It was then cooled to ambient temperature and stored in a desiccator. This pre-treatment was also recreated in a TGA instrument, where the petcoke was heated and then cooled down in a N_2 flow, followed by CO_2 gasification. The similarity in the devolatilised and raw petcoke mass loss curves during the gasification step confirmed that the devolatilization and the cooling steps introduced due to the pretreatment did not significantly affect the gasification of the material (Supplement S2). Moreover, the test with the non-devolatilised petcoke was carried out in the main test rig under the most reactive of the studied conditions, and a comparison is presented in Supplement S3. An initial, rapid loss of approximately 10% of the sample mass occurred due to the rapid release of volatiles; however, the further mass loss curve was parallel to that of the devolatilised sample, and the reactivity at 50% conversion (R_{50}) was 0.023 and 0.022 (1/min) for non-devolatilised and devolatilised petcoke, respectively. Therefore, it can be assumed that the relatively slow gasification reaction was not affected by the rapid release of lighter compounds at the beginning of the process and that the devolatilization time was negligibly small compared with the oxidation of the solid residue. Therefore, the applied petcoke pre-treatment should not affect the kinetic parameters obtained in this research.

2.2. The test rig and experimental procedure

Petcoke gasification kinetics were determined from a series of measurements performed in the custom-built test rig for thermochemical fuel conversion studies (Fig. 1). The test rig can operate in two modes, referred to as the gravimetric and evolved gases methods. The main principle of the experiment was to perform the gasification of petcoke under isothermal conditions in a controlled flow of a gaseous mixture with a predetermined composition while registering the mass loss of the sample during the reaction. The decrease in the sample mass was determined by directly measuring the sample's weight during the reaction (gravimetric method). For some tests, the mass loss was validated by calculating the amount of carbon in the gases produced during petcoke gasification in another configuration of the test rig, where the gaseous products were monitored instead of the mass of the sample (evolved gases method).

Pictures of the test rig are shown in Fig. 1. The main part of the rig is comprised of two electrical furnaces fixed on a common panel attached to a vertical rail. An electric motor (1) allows for a rapid (*ca.* 300 mm/s) movement of the panel along the rail over a distance of 500 mm to quickly heat the sample (*ca.* 1700 □/min). The required gas mixture of $N_2/CO_2/O_2$ was prepared by supplying high-purity (99.999 %) gases from gas cylinders into the mixing chamber (2) using thermal mass flow controllers. Since some of the examined gasification parameters requires steam, the gaseous mixture is supplied to the separate quartz tube reactor, the evaporator (3), before entering the reaction zone. If steam is required, a constant water flow is delivered to the evaporator using a syringe pump (4) and a PTFE transfer line, inserted from the bottom of the reactor and nested in a quartz wool plug, in the middle of the heating zone of the evaporator. The temperature in the evaporator is maintained at 300 □ to ensure constant, complete water vaporisation. The gases from the cylinders, now mixed with the steam, are further transferred via a heated line (5) into the main reactor, enclosed in the second furnace (6).

Depending on the selected method, one of the two types of vertical quartz tube reactors can be fixed in the furnace of the test rig. For the gravimetric method, a reactor (i.d. 27 mm) sealed at the top and opened at the bottom was used. The gaseous mixture was continuously supplied to the top of the reactor. Below the open lower end of the tube, a weighing module (7) enclosed in a protective case and purged with a constant N_2 flow was placed. A quartz rod was attached to the weighing plate of the module. The shift of the panel with the furnaces to the lowest position allowed the rod to be inserted into the reactor through its open end. At the end of the rod, in the middle of the reactor heating zone, a quartz sample holder (8) is mounted. The holder is cylindrical with an i.d. of 15 mm and a bottom made of a G3 quartz frit disc to allow the gaseous mixture to pass through the bed of the sample. The gaseous mixture and evolved gasification products exit the reactor through the open end. The sample mass was continuously measured, with the accuracy of 0.1 mg, throughout the experiment.

The second method, involving analysis of the released gases, required an air-tight gas outlet from the reactor; thus, it is impossible to register sample mass during this measurement. In this mode, a quartz tube (i.d. 20 mm) sealed on both ends is used, and the gaseous mixture is also supplied to the top of the reactor. It passes through a fixed bed of sample that is placed in the middle of the heating zone and is supported by a quartz wool plug. Through the sealed bottom end of the reactor, a thermocouple enclosed in a protective quartz tube is inserted to monitor the temperature of the bed. The evolved gases are transferred from the reactor through a cleaning line directly to the sampling loop of a gas chromatograph with a thermal conductivity detector (GC-TCD). The cleaning line includes an isopropanol impinger to remove condensable species, a particular matter filter, and a moisture trap. Gases, which constantly purged the sampling loop of the GC-TCD, were analysed every 10 min by switching the 6-way valve, which introduced the current contents of the sampling loop into the capillary column. The analysis was performed with an Agilent 6890N gas chromatograph

with a TCD detector, with the 100 ppm limit of quantitation. The samples were separated on a capillary J&W GS-CarbonPLOT 30 m x 0.53 mm x 3 μm column followed by J&W HP-PLOT 30 m x 0.53 mm x 25 μm molecular sieves. For the duration of CO_2 elution, the latter was bypassed using a 6-way valve.

Fig. 1. Test rig for petcoke gasification in the gravimetric mode with the furnace in the lower (left) and upper (right) position (1 – electric motor, 2 – gaseous mixture preparation unit, 3 – evaporator, 4 – syringe pump, 5 – heated transfer line, 6 – the main furnace, 7 – weighting module, 8 – sample holder)

The measurement principles of both methods are detailed in Fig. 2. In the gravimetric method, 300 mg of the sample (20 mg in tests with O_2 to limit diffusion resistance) was weighted into the crucible attached to the rod connected to the weighing module, while the furnace panel was in the upper position, so that the reactor was above the sample holder. The experiment

can be carried out with either a low or high heating rate. In the former case, the furnace panel is lowered prior to heating, and the sample is therefore enclosed inside the reactor purged by a N_2 flow. The furnace is then heated to the selected temperature at a rate of 20 □/min. The atmosphere is then switched to the predefined gaseous mixture and the gasification process is initiated. The mass loss in time is registered, providing the process kinetics data. A high heating rate of *ca.* 1700 □/min could be achieved by lowering the pre-heated furnace so that it rapidly enclosed the sample that was waiting in the ambient atmosphere. However, only preliminary tests are carried out using the fast heating, while the main experiments used for kinetic calculations were performed using the slow heating. The comparison of tests at both heating rates (presented in Supplement S4) revealed that, although the initial mass loss of the sample slightly increased during rapid heating, the average reactivity (R_{50}) during conversion was not significantly affected by the sample heating time, due to the relatively long total gasification time.

In the gas evolution method, the gasification products are determined using GC-TCD analysis. The test rig setup included a sealed gas-tight reactor (Fig. 2). A 500 mg sample was enclosed in the reactor prior to the experiment and purged with N_2, while the reactor was heated with a controlled, low heating rate (20 □/min) up to the desired temperature. The N_2 flow was then switched to the gasification mixture and the online analysis of the gasification products, in 10 min intervals, was initiated.

a) b)

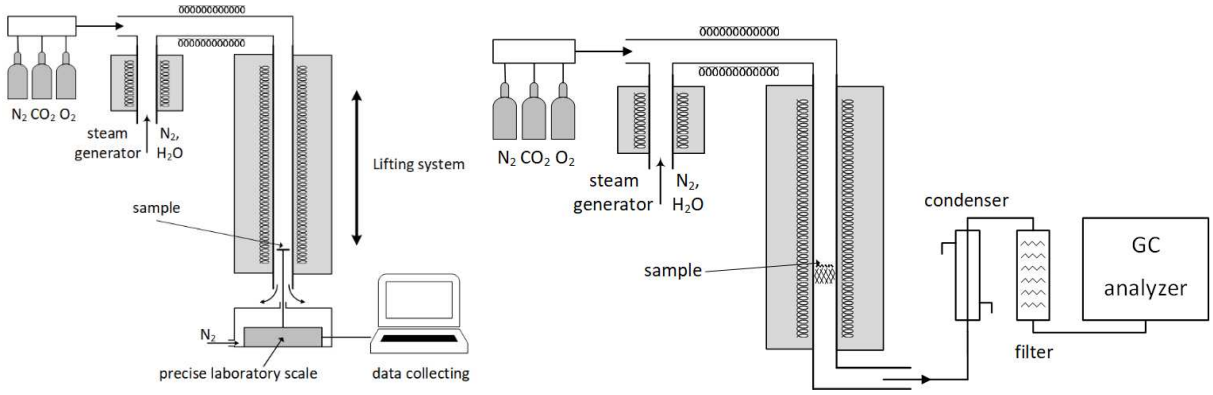

Fig. 2. The principle of petcoke gasification with the a) gravimetric and b) evolved gases methods

The parameters for the petcoke conversion tests were selected to represent the conditions in a commercial CLC gasification unit. Therefore, the experiments were carried out under atmospheric pressure at temperatures in the range of 750 – 1100 ℃ and the oxidising agent concentrations set to: 2 and 4 vol.% for O_2; 10 and 40 vol.% for CO_2; and 10, 20 and 40 vol.% for H_2O.

2.3. Calculations

Kinetic parameters are calculated only from the mass loss curves obtained from the gravimetric method. The evolved gases mode was mainly used to evaluate the reaction products; however, the mass loss of petcoke during steam gasification is also estimated from the carbon balance, based on all detected carbon-containing species, i.e. CO, CO_2, and CH_4. The remaining relative mass of the sample is expressed as:

$$m_{\mathrm{rel}}(t) = 1 - \frac{\left(n_{CO}(t) + n_{CO2}(t) + n_{CH4}(t)\right)M_C}{m_i x_c} \quad (1)$$

where n_i is the integrated molar amount of carbon (in mmol) in the *i*-th reaction product released in the time interval from $t = 0$ to $t = t$, M_C is the carbon molar mass (in mg/mmol), m_i is the initial mass of petcoke (in mg), and x_c is the mass fraction of C in petcoke (in mg C/mg).

The recorded mass losses during the gravimetric method are used to calculate the carbon conversion, which is defined as

$$X(t) = \frac{m_0 - m(t)}{m_0 - m_\infty} \tag{2}$$

where m, m_0 and m_∞ are the instantaneous, initial and final masses of the sample, respectively (in mg). In the experiments where full conversion was not reached, the final mass was assumed based on the residual mass obtained in the tests with complete sample conversion.

A general form of the apparent rate of conversion for gas-solid reactions is given by

$$\frac{dX}{dt} = k f(X) p_{ox}^n \tag{3}$$

where p_{ox} is the partial pressure of the oxidizer (Pa), n is the reaction order, k is the apparent reaction rate coefficient (in 1/(s·Pa^n)) and $f(X)$ is a model function. The apparent reaction rate coefficient k takes into account the changes in temperature introduced in the Arrhenius form

$$k = A \exp\left(-\frac{E}{RT}\right) \tag{4}$$

where A is the pre-exponential factor (in 1/(s·Pa^n)), E is the activation energy (kJ/mol), R is the universal gas constant (in kJ/(mol·K)) and T is the temperature (in K). The model function

$f(X)$ takes into account variations in the physical and chemical properties of the sample as the reaction proceeds. Four model functions are tested within this study. First is the uniform conversion model [29], also known as homogeneous [30] or Avrami model (AVRAMI) [31], which is given by

$$f(X) = (1 - X) \tag{5}$$

The second examined function is the Random Pore Model (RPM) [31][32] expressed as

$$f(X) = (1 - X)\sqrt{1 - \psi \ln(1 - X)} \tag{6}$$

where ψ is the pore structure parameter, which can be determined using

$$\psi = \frac{2}{2\ln(1 - X_{max}) + 1} \tag{7}$$

where X_{max} is the conversion at maximum reaction rate, which is determined using the condition

$$\frac{d(dX/dt)}{dX} = 0 \tag{8}$$

The third considered model function is the Shrinking Core Model (SCM) [31]

$$f(X) = (1 - X)^m \tag{9}$$

where $m = 2/3$ for spheres is assumed. The last function analyzed is called the Hybrid Model (HM) [31] which is identical to Eq. (9), but the exponent m is treated as a parameter and is adjusted during data fitting.

The experimental data is analysed using a series of scripts written in Matlab. As mentioned earlier, the measurements are done for petcoke reactions with O_2, H_2O and CO_2. For all reactants, the reaction orders n were determined first, by analysing the conversion rates

obtained for various partial pressures of the reactants. Then, the obtained reaction orders were kept constant and the reaction rate coefficients were determined by fitting the conversion rates with functions (5)-(9). Finally, the kinetic parameters A and E from Eq. (4) were determined using Arrhenius plots. The results of the analyses are presented in section 3.2.

3. Results and discussion

3.1. Results of the petcoke gasification experiments

3.1.1. Gas evolution profiles

Gases released during the gasification of petcoke in 10 and 40 vol.% of steam in N_2 were measured online with a gas chromatograph coupled with a thermal conductivity detector (GC-TCD). The evolution profile for the test performed at 1000 □ in 40 vol.% of steam in N_2 is presented in Fig. 3 as an example; the main released gases were CO and H_2, while the CO_2 and CH_4 yields were an order of magnitude lower. The delayed increase in the CO_2 evolution profile suggests that the water-gas shift (WGS) reaction was intensified during gasification. This could be due to either the catalytic effect of metals exposed by the initial carbon consumption with steam or as a result of a local increase in the steam concentration in the particle's surrounding, which occurred as the main steam gasification reaction, responsible for CO formation, slowed after 50 min. Another explanation for the delayed release of CO_2 might be its chemisorption on the petcoke surface at the initial stage of the process. For all examined cases, the maximum H_2 and CO yield occurred around the 0.1 conversion, and reaching even this early stage of petcoke gasification required residence times too long to be considered in operating commercial reactors. However, the experiments with steam as a sole oxidising agent were performed for the purpose of kinetic parameters determination that will be implemented in the modelling of a real gasifier. Due to the low reactivity of the sample, and

the limited duration of the experiment (480 min), the carbon conversion, X, in the tests with the lower steam concentration reached only 0.5 – 0.75, depending on the applied temperature. Thus, the composition of the gaseous products was averaged only for the first half of the petcoke conversion (up to $X = 0.5$), and the result is presented in Fig. 4. As can be seen from the figure, CO and H_2 were the main gasification products, and their yields peaked at the beginning of the process and then decreased continuously with the carbon burnout. The molar ratios of the cumulative amounts of H_2 and CO (n_{H2}/n_{CO}) released during carbon conversion up to $X = 0.5$ at temperatures up to 1000 □ were between 1.2 – 1.4 for the gasification with steam. The CO_2 concentration in the gasification products (i.e. excluding N_2 and H_2O) was below 5 vol.%. The composition of the obtained syngas was similar to the values reported by Trommer et al. [33] for two petcoke samples gasified in 10 vol.% steam in a plug flow reactor. However, more CO_2 was formed under the most reactive conditions, i.e. 40 vol.% of steam and 1100 □. Wu et al. [9] stated that during petcoke gasification with steam in a fixed-bed reactor the water-gas shift reaction (WGS) shown in equation 10 will not reach equilibrium.

$$\mathrm{CO + H_2O = CO_2 + H_2} \tag{10}$$

Since the WGS reaction rate increases rapidly above 1000 ℃, at 1100 ℃ the WGS reaction is intensified, despite its exothermic character, while the rate of the heterogenous reaction

$$\mathrm{C + H_2O = CO + H_2} \tag{11}$$

is constrained by the available surface of the petcoke particles, which increases CO_2 and decreases CO yield. Another possible explanation for the observed increase in the CO_2 formation is the rapid increase in the catalytic activity of the metal M-C-O conformations in petcoke, which are known to increase selectivity towards CO_2 formation, at the expense of CO yield [9,34].

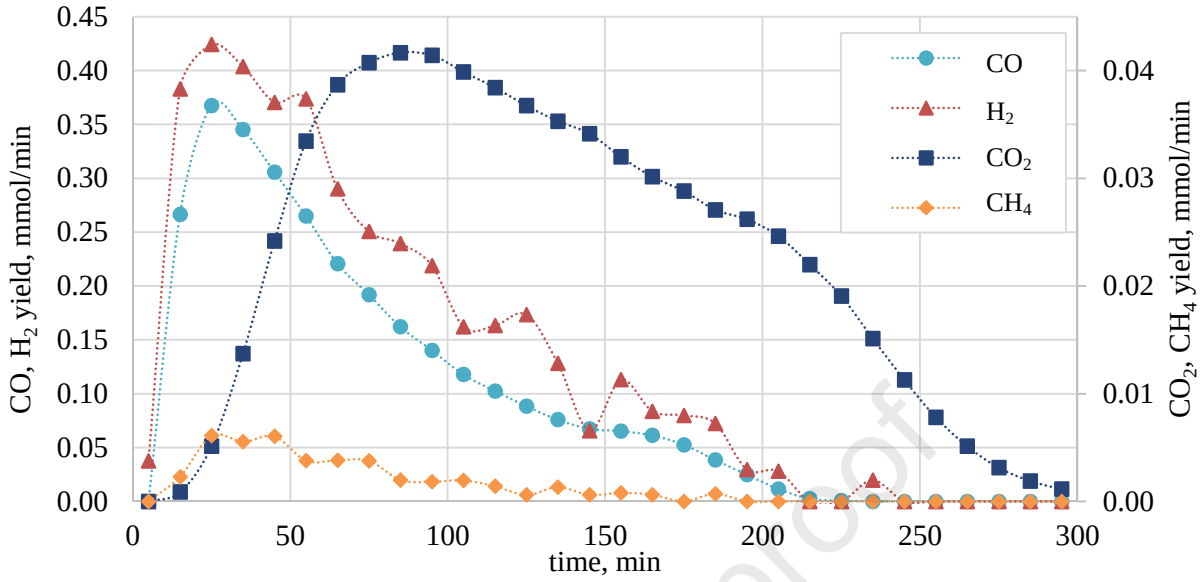

Fig. 3. Gas evolution profiles for petcoke gasification in 40 vol.% of steam in N_2 at 1000 □

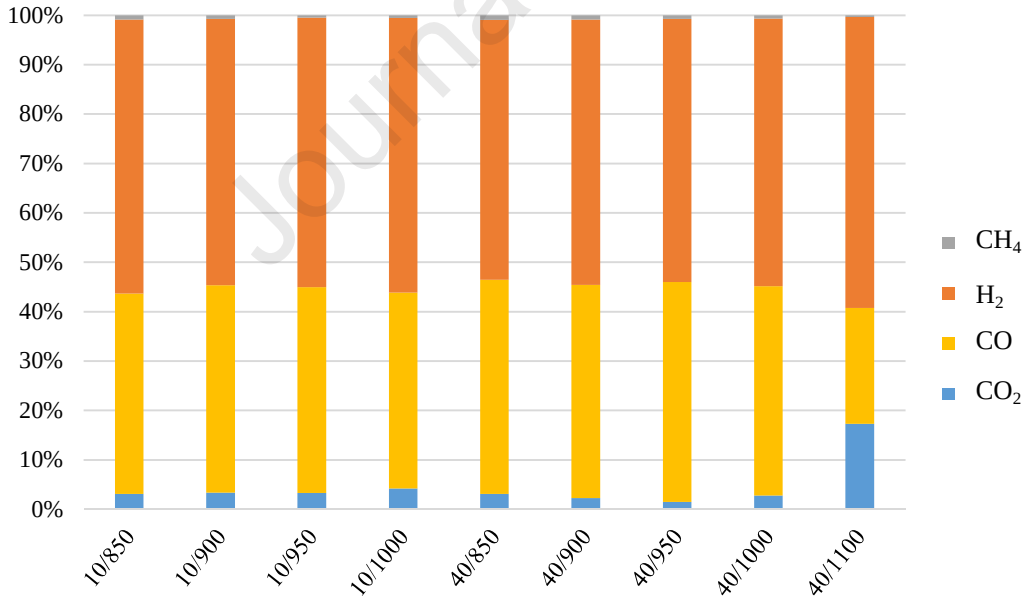

Fig. 4. Composition of the gaseous reaction products from petcoke steam gasification averaged for the conversion $X = 0$ to $X = 0.5$ (labels: *steam concentration in vol.%/reaction temperature in* □)

As can be seen from Fig. 5, the reaction rate of petcoke gasification with CO_2 was extremely slow. The measurement time was arbitrarily limited to 480 min and negligible conversion was achieved during these tests. Gasification with CO_2 gradually increased the porosity of petcoke, resulting in an increase in the CO yield. Even under the most reactive condition, i.e. 40 vol.% of CO_2 at 1000 □, the reaction rate did not reach its maximum even after 480 min of measurements, while, in the same concentration of steam, the petcoke bed reached full conversion in less than 240 min. Therefore, the role of CO_2 during petcoke gasification below 1000 □ could be considered negligible and it does not have any applicable commercial value. Since the petcoke conversion with CO_2 was so slow, realistic kinetic parameters could not be obtained.

In contrast, petcoke gasification in 4 vol.% of O_2 was very rapid. In the temperature range of 750 – 1000 □ total conversion was reached in less than 15 min. Since the online gas analysis with GC-TCD was performed in 10 min intervals, no evolution profiles could be determined from these tests. The kinetic parameters of oxygen conversion were, therefore, determined based on the gravimetric tests. The only detected reaction product was CO_2, which suggest that the combustion of petcoke was complete.

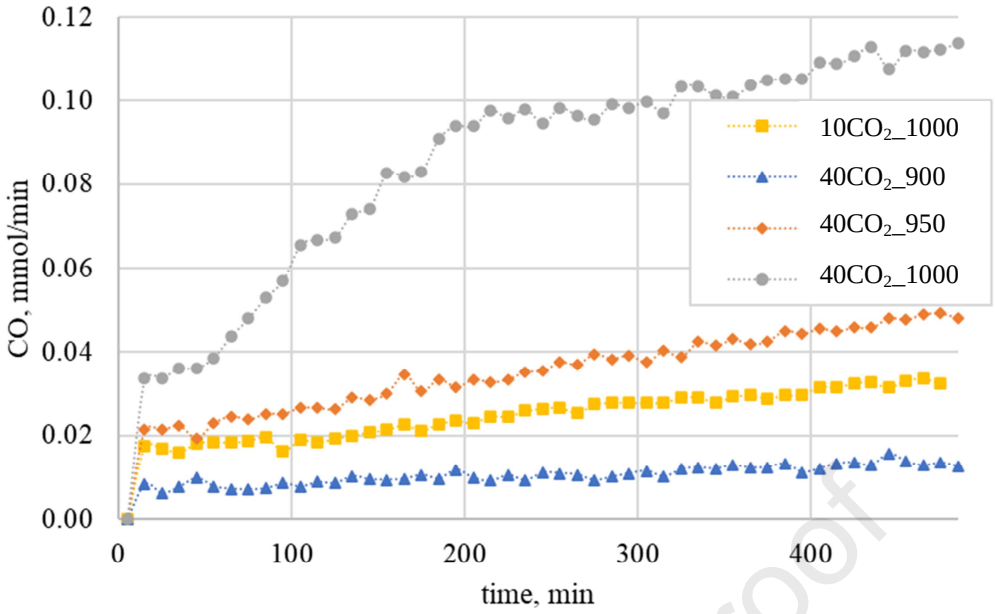

Fig. 5. CO released during 480 min of petcoke gasification in 10 vol.% and 40 vol.% of CO_2 in N_2 at 900, 950 and 1000 □

3.1.2. The results of the gravimetric and evolved gases experiments

Gravimetric analysis of petcoke gasification in steam and in oxygen was used to calculate kinetic rate parameters for the heterogeneous reactions. In addition, for steam gasification, gas evolution profiles were also used to determine the corresponding mass loss curves. This was done based on the amount of carbon in the gaseous reaction products (Eq. 1). The comparison of the mass loss functions obtained with both methods is presented in Fig. 6 and Fig. 7 for experiments performed in 10 vol.% and 40 vol.% of steam, respectively.

At the lower steam concentration, and thus a lower reaction rate, the curves were similar, but some discrepancies can be seen for the reactions carried out under more reactive conditions. For those cases where full conversion was reached within the time frame of the experiment, i.e. where $dX/dt = 0$ at the end of the experiment, the final conversion found from the EV

method is 0 – 0.1 larger than for the GR method. This discrepancy may be because not all gases were correctly captured and integrated using the EV method. For these cases, the final conversion of the EV method is normalised by the one obtained using the GR method. A relatively good agreement between the mass loss plots obtained with EV and GR methods suggests that the former provides valid data on the composition of released gases and can be applied to study the petcoke gasification mechanisms and kinetics. As no solid deposits were observed in the experiments, the differences between the methods may result from the larger uncertainties of the indirect mass loss determination approach of the EV method; thus, the data from the GR method was used for the kinetic parameter calculations. This observation indicates that no such limitation occurs at lower temperatures, thus the kinetics calculated from the petcoke gasification experiments up to 950 □ can be attributed to the chemical reaction rates and increase in the surface area of the particles, rather than diffusional limitations of a fixed bed.

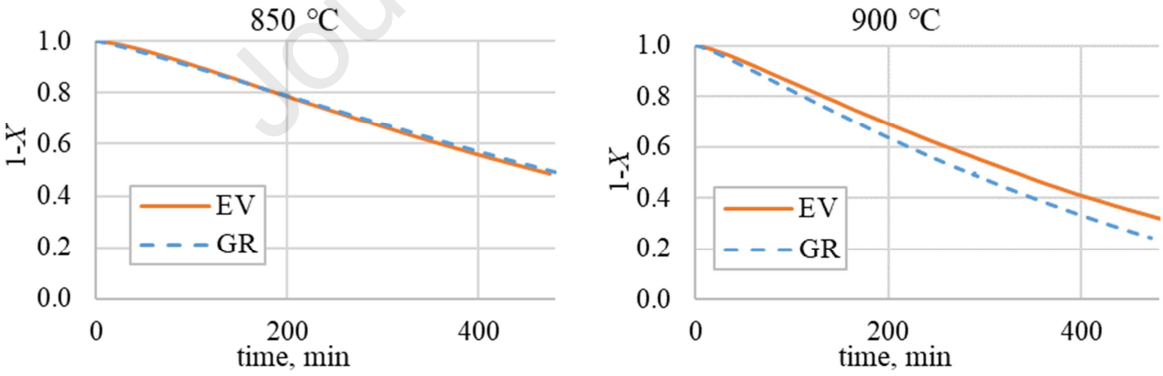

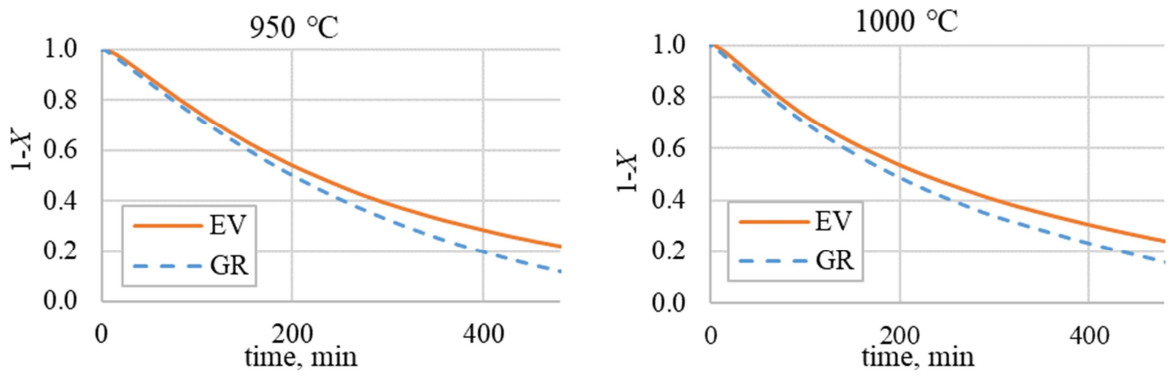

Fig. 6. Mass loss curves from gravimetric (GR) and evolved gases (EV) analysis of petcoke gasification in 10 vol.% of steam in N_2

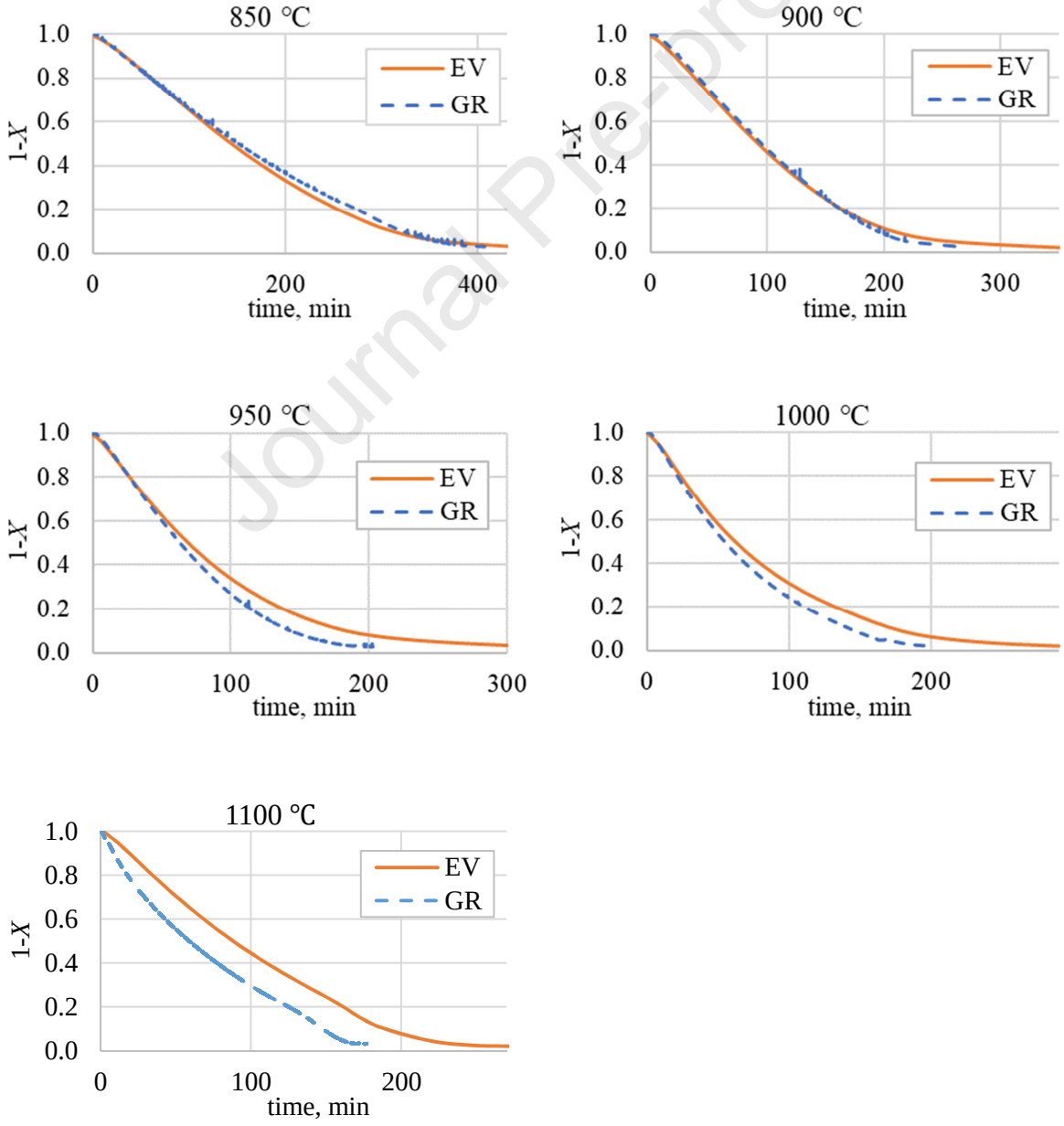

Fig. 7. Mass loss curves from gravimetric (GR) and evolved gases (EV) analysis of petcoke gasification in 40 vol.% of steam in N_2

The mass loss curves from the gravimetric tests of petcoke gasification with 2 and 4 vol.% of O_2 are presented in Fig. 8. As expected, the reaction occurs more rapidly at higher temperatures. CO_2 is the only detected product, and the higher oxygen concentration significantly shortens the reaction times.

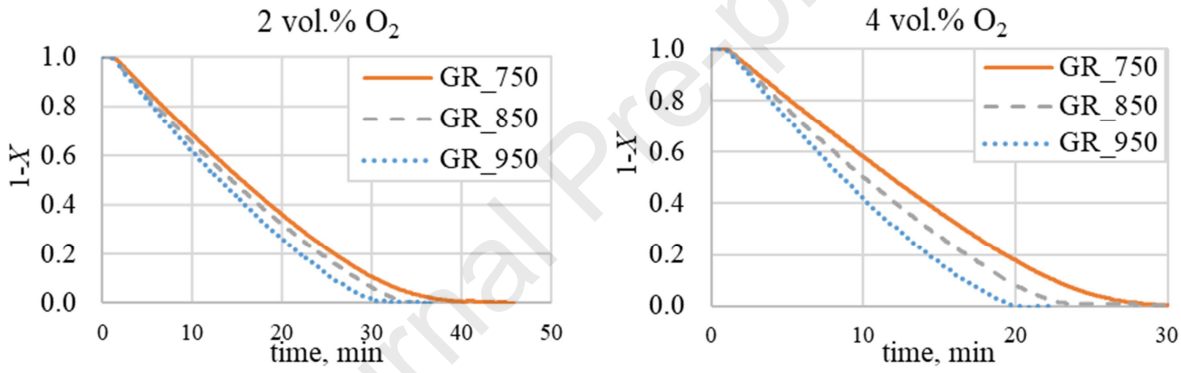

Fig. 8. Mass loss curves from gravimetric analysis of petcoke gasification in 2 and 4 vol.% of O_2 in N_2

3.1.3. Petcoke gasification in a mixture of steam and CO_2

The reaction of petcoke with CO_2 was significantly slower than steam gasification; nonetheless, a possible contribution of CO_2 during petcoke conversion under the more complex gasification atmosphere was examined by performing tests in a mixture of 40 vol.% of H_2O in CO_2. The results were compared with the steam gasification measurements using inert N_2 as the carrier gas, as presented in Fig. 9. The mass loss registered during the 480 min

conversion tests in 40 vol.% of CO_2 in N_2 are also provided as a reference. It can be noted that, up to 1000 □, the curves of the petcoke mass loss during reactions with 40 vol. % of steam were not affected by changing the carrier gas from N_2 to CO_2. This finding confirmed the dominating role of H_2O over CO_2 in the petcoke gasification process at these temperatures. However, the reaction with CO_2 became significant at 1100 □. At the same time, since full conversion was reached for steam gasification (after about 160 min), almost 1/3 of the sample was converted when H_2O was substituted with CO_2. The same non-negligible role of CO_2 at high temperatures was confirmed by the enhanced petcoke conversion when N_2 was substituted with CO_2 for the measurement at 1100 □. Therefore, for high-temperature petcoke gasification the presence of CO_2 should be accounted for, while it can be disregarded under less-reactive conditions.

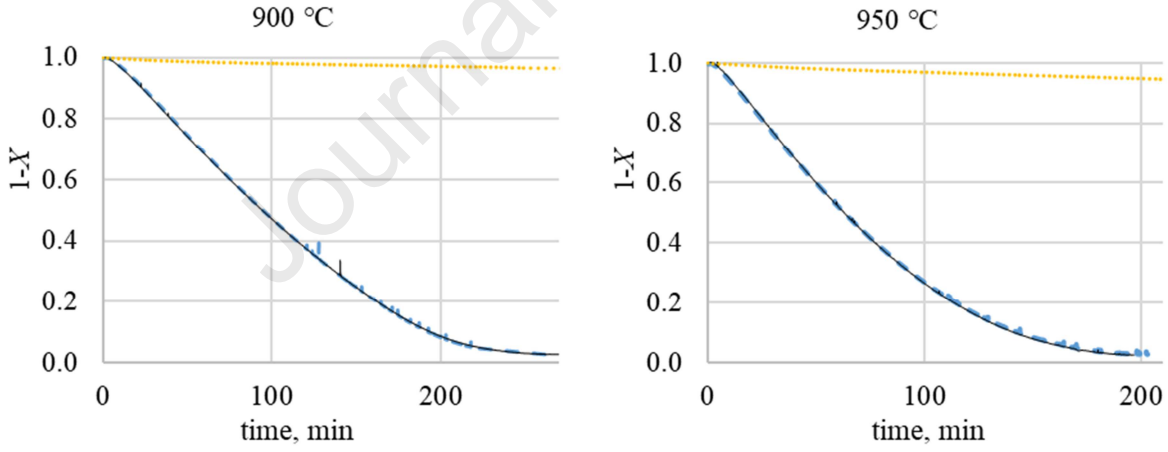

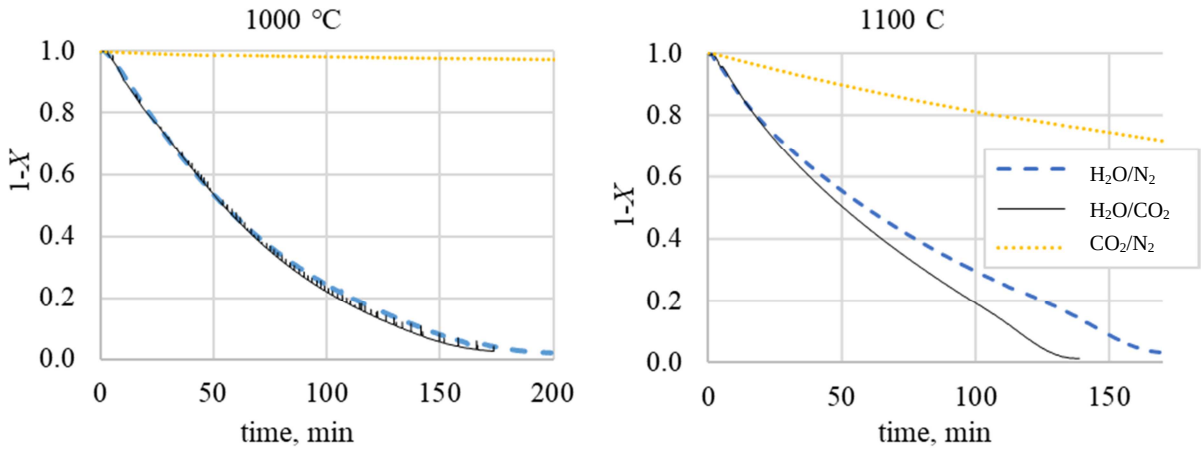

Fig. 9. Mass loss of petcoke during gasification in 40 vol.% of H_2O with N_2 and CO_2 as the carrier gas and in 40 vol.% of CO_2 in N_2

Petcoke gasification measurements in 20 vol.% steam in CO_2 were also carried out at temperatures up to 1000 □. From these results, the assumption that the type of the carrier gas does not affect the kinetics of the steam gasification of petcoke in this temperature range was confirmed by comparison with corresponding measurements in H_2O/N_2 atmospheres.

Moreover, using 20 vol.% of steam for these additional tests allowed validation of the results of the models applied for the conversion in 10 and 40 vol.%. The mass loss of petcoke in 40, 20 and 10 vol.% of steam (in either N_2 or CO_2) is presented in Fig. 10. Steam concentration had a strong impact on the petcoke gasification, and when a higher steam content was used, the total conversion times were shorter, regardless of the applied temperature. At 900 □, the gasification reaction was significantly slower for all examined steam concentrations. However, the offset between the mass loss curves at 950 and 1000 □ was less pronounced and decreased with the reaction time. Surprisingly, after reaching 0.6 and 0.9 conversions with 20 and 10 vol.% of steam, respectively, the remaining mass of petcoke was lower at 950 □ than at 1000 □, possibly due to diffusional limitations at 1000 □.

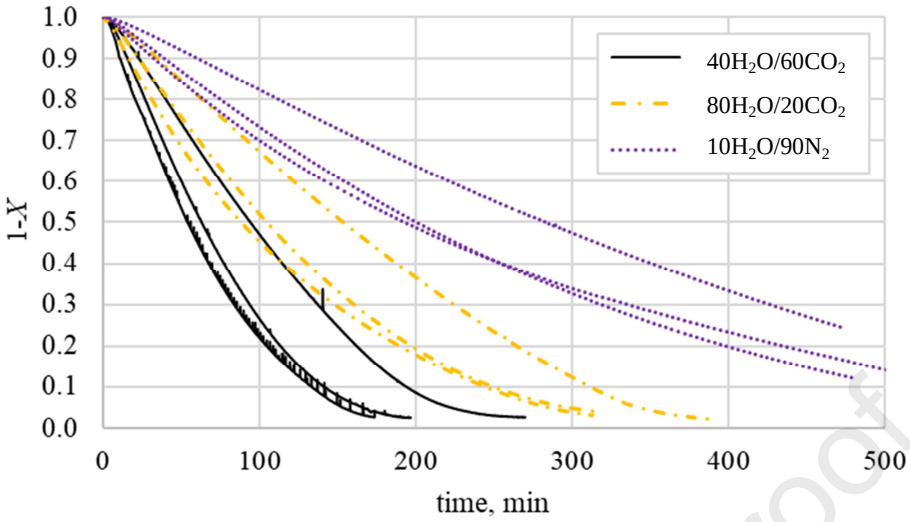

Fig. 10. Mass loss of petcoke during gasification in 40, 20 and 10 vol.% of steam at 900, 950 and 1000 □

3.2. Calculation of the kinetic parameters of petcoke gasification

3.2.1. Reaction with O_2

Petcoke oxidation experiments in an O_2/N_2 mixture were performed for two O_2 concentrations of 2 and 4 vol.% and three temperatures of 750, 850, and 950 ℃. The obtained conversion curves are presented in Fig. 11. To determine the reaction order the reaction rates (dX/dt) vs. conversion (X) were limited to the regions of $X\epsilon < 0.2, 0.8 >$ in which straight lines were fitted to the data, as presented in Fig. 12, following the procedure described by Gartner et al. [31]. The reaction orders were then determined from a plot of $\ln(dX/dt)$ vs. $\ln(p_{O2})$ for each conversion X, and based on the obtained results, a mean reaction order was calculated. For the reaction with O_2 the determined mean reaction order is n=0.55. It should

be stressed, however that variations in the reaction order n with conversion X were observed, in the range from 0.42 to 0.66.

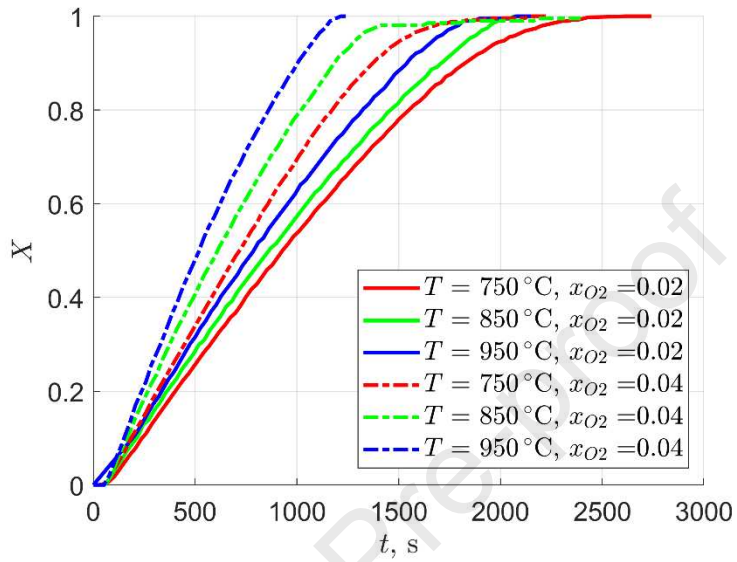

Fig. 11. Experimentally determined fuel conversion vs. time for two different mole fractions of oxygen

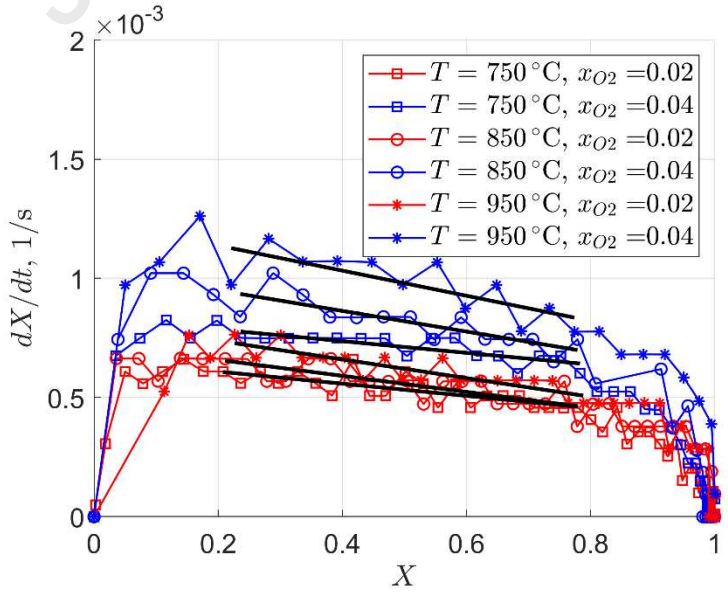

Fig. 12. Linear fits to the experimental data for reaction order determination

The mean reaction order was then used to calculate the apparent reaction rate coefficient k (and m for HM) by fitting the experimental data with the models defined in Eqs (5) – (9). In Fig. 13, the $f(X)$ function models fitted to the experimental data are compared. As can be seen, the best fit was obtained for the Hybrid Model (HM), which was confirmed by comparison of the sum of squared residuals SSR defined as

$$SSR = \sum_{i=1}^{N} (\varepsilon_i)^2 \tag{12}$$

where ε_i is the residual (the difference between experimental data and model) and N is the number of data points. The SSR for each model for all temperatures, as presented in Fig. 13, are: AVRAMI $SSR = 4.0 \cdot 10^{-6}$, RPM $SSR = 1.4 \cdot 10^{-6}$, SCM $SSR = 1.7 \cdot 10^{-6}$, HM $SSR = 1.8 \cdot 10^{-7}$.

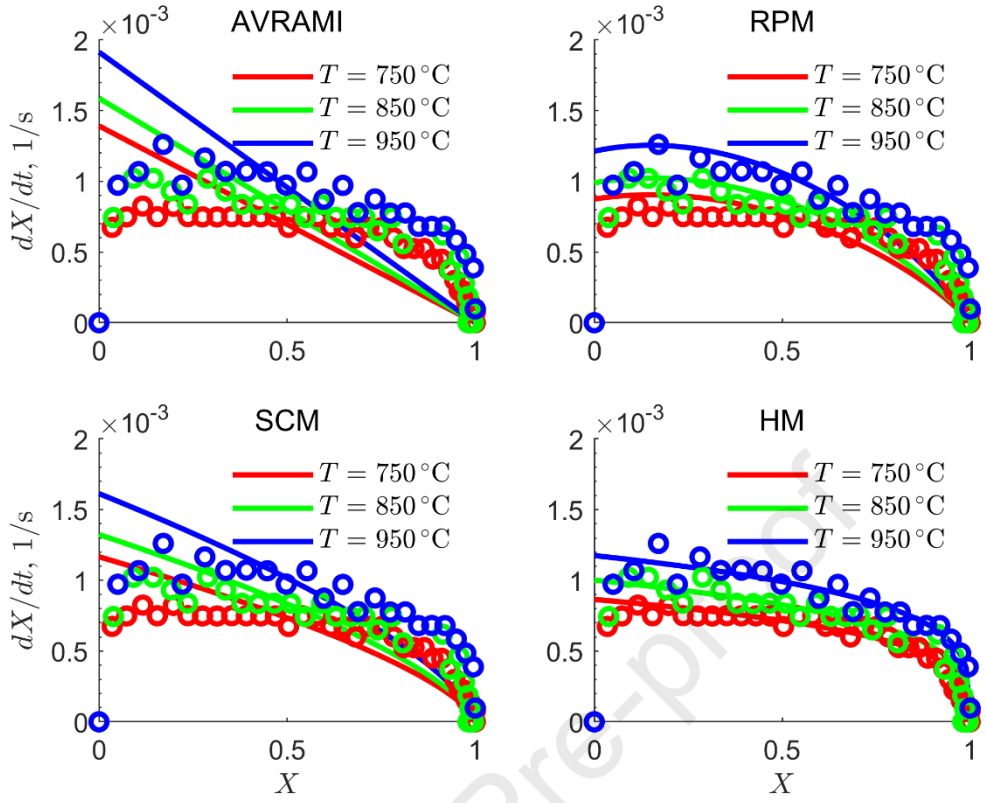

Fig. 13. Comparison of fitted model functions $f(X)$ for the reaction with O_2 ($x_{O2} = 0.04$)

Finally, the calculated apparent reaction rate coefficients k were used to determine the pre-exponential factor A, and the activation energy E, by fitting the plotted $\ln(k)$ vs. $1/T$ data, as presented in Fig. 14. The fitted linear functions predicted the obtained rate coefficients well, suggesting that the reactions occurred in the kinetic regime, as required by the tested models. The determined model parameters are summarised in Table 1. The obtained model parameters were then used to verify the model predictions by integrating the conversion rates (dX/dt) for the various models and comparing the results with the experimentally determined conversions. The comparison is presented in Fig. 15. The AVRAMI model was excluded, as it gave the poorest predictions. All models predicted the experimentally-determined petcoke conversion vs. time. In some instances, the models slightly overpredicted the conversion, which is associated with the observed initial time delay of the conversion due to initial sample heating up not captured by the models. In general, the best predictions were obtained for the

Hybrid Model (HM), which is confirmed by the lowest residuals. The calculated sums of squared residuals (SSR) were: RPM $SSR = 1.3 \cdot 10^{-5}$, SCM $SSR = 2.2 \cdot 10^{-5}$, HM $SSR = 1.2 \cdot 10^{-5}$. Therefore, it is recommended to use the Hybrid Model (HM) for reactions with O_2. It should be also stressed that the models are valid in the kinetic regime.

It was reported by Afrooz et al. [35] that the activation energy of petcoke oxidation decreased from 124 to 35.3 kJ/mol (determined with SCM), and from 124.8 to 31.3 kJ/mol (determined with RPM) when heating rate in the TGA program was increased from 10 to 20 K/min. In this work, the sample was already at the reaction temperature when the oxidising agent was introduced, thus, it is plausible, that the lack of the heating step further decreased the activation energy to the values calculated hereby.

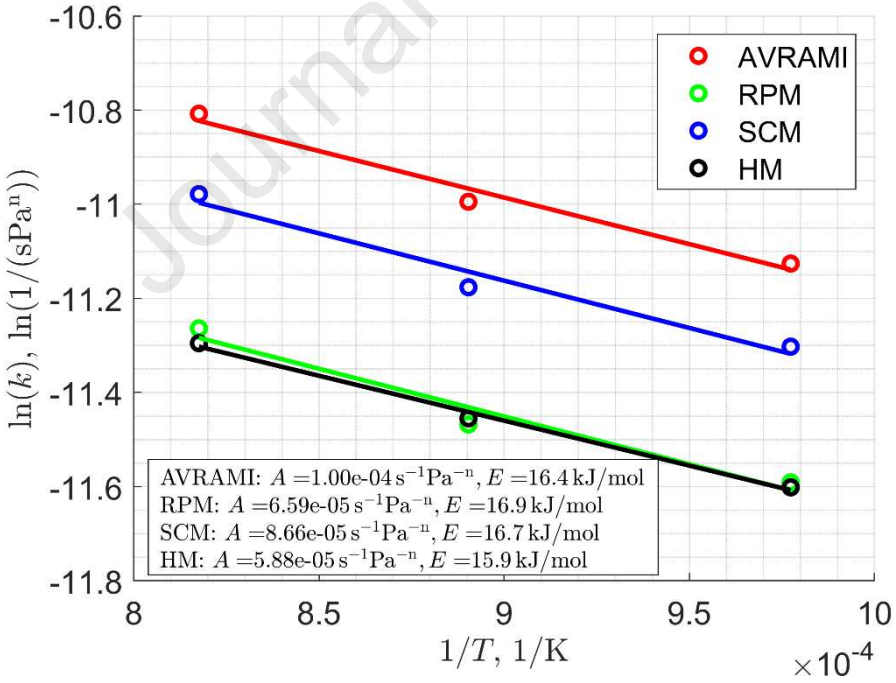

Fig. 14. Determination of the pre-exponential factor A and activation energy E

Table 1: Summary of the model parameters determined for the reaction of petcoke with O2

Model	Equation* $\frac{dX}{dt} = A\exp(-E/RT)f(X)p_{O_2}^n$	A $1/(\mathrm{sPa}^n)$	E kJ/mol	n	m	ψ
AVRAMI	$f(X) = (1-X)$	1.004e-4	16.44	0.548	-	-
RPM	$f(X) = (1-X)\sqrt{1-\psi\ln(1-X)}$	6.595e-5	16.85	0.548	-	2.963
SCM	$f(X) = (1-X)^m$	8.660e-5	16.70	0.548	0.667	-
HM**	$f(X) = (1-X)^m$	**5.875e-5**	**15.87**	**0.548**	**0.266**	-
*p_{O2} in Pa, T in K; **recommended model						

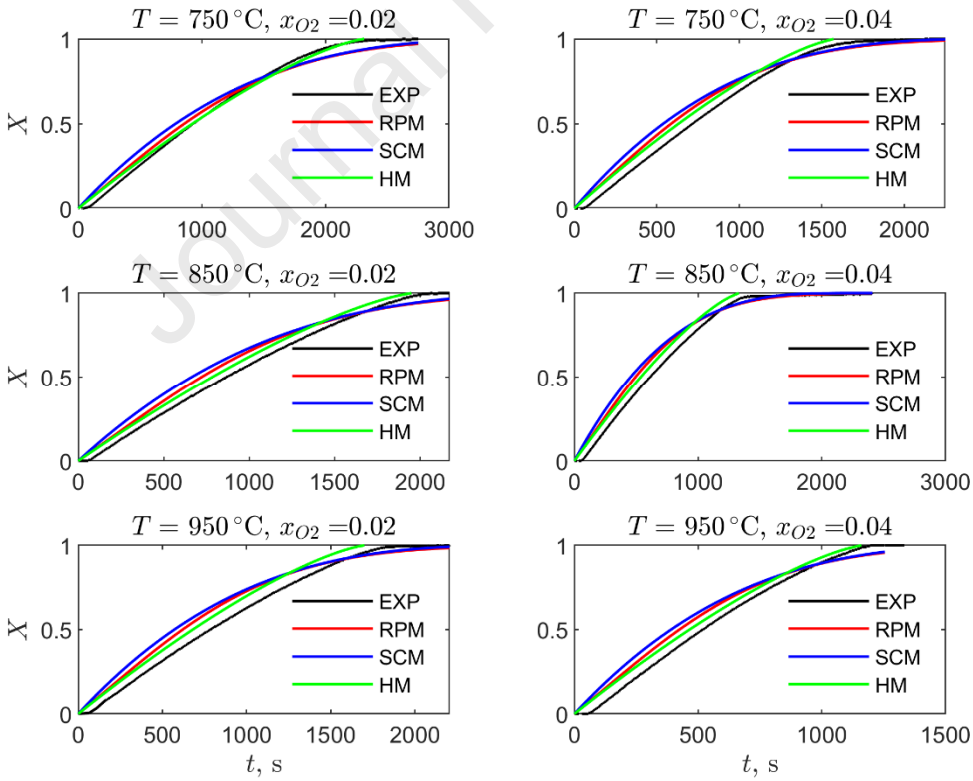

Fig. 15. Comparison of experimental data (EXP) and predictions of the subsequent models

3.2.2. Reaction with H_2O

The same procedures for determining the kinetic parameters as described above for O_2 were applied for the reaction with H_2O, where the petcoke was gasified in a H_2O/N_2 mixture for the two H_2O concentrations of 10 and 40% vol. In Fig. 16, the experimentally-determined fuel conversion vs. time is presented. As can be seen, the conversion lines cross for the high temperature tests. These phenomena are attributed to the reaction rate reduction due to diffusion at high temperature. Furthermore, not full conversion was obtained at the H_2O concentrations of 10 vol.% due to very long reaction times. It should be however stressed that both concentrations ($x_{H2O} = 0.1$ mol/mol and $x_{H2O} = 0.4$ mol/mol) and all temperatures were used to determine the reaction order. For the determination of the kinetic parameters, only data for low temperatures and high H_2O concentrations ($x_{H2O} = 0.4$ mol/mol) were used. In general, large variations in the reaction orders with temperature was observed, and a mean value of $n = 0.9$ was calculated and used. Another choice would be to take the orders for low temperatures (n ~ 0.86). Since the value was close to the one for all temperatures and the fitted model predictions with an order of 0.9 were satisfactory, this approach was used, and four models (AVRAMI, RPM, SCM and HM) were tested as previously. In Fig. 17, a comparison of the fitted model functions $f(X)$ to the experimental data is presented. As can be seen for the highest temperature of 1000 ℃, the reaction rate is initially the highest, however at conversions greater than 0.5, the reaction rate decreases below that of the 950 ℃ plot.

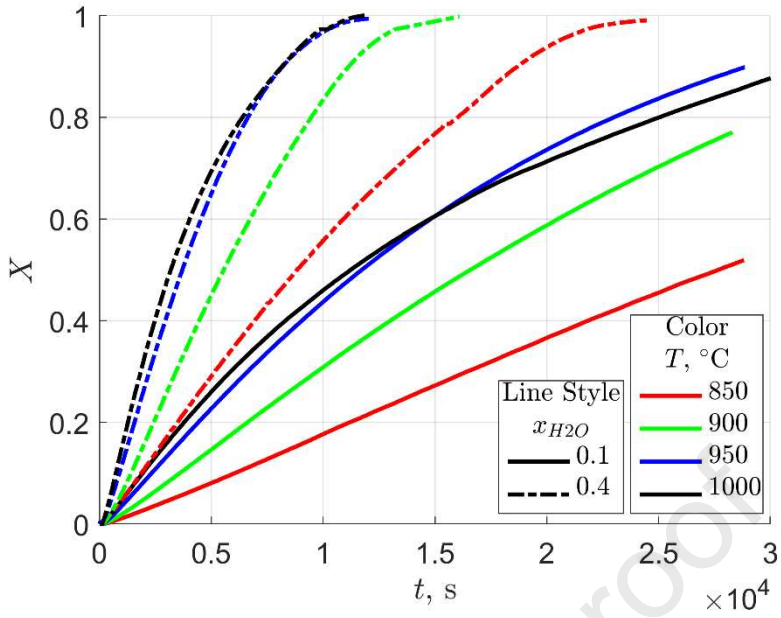

Fig. 16. Experimentally-determined fuel conversion vs. time

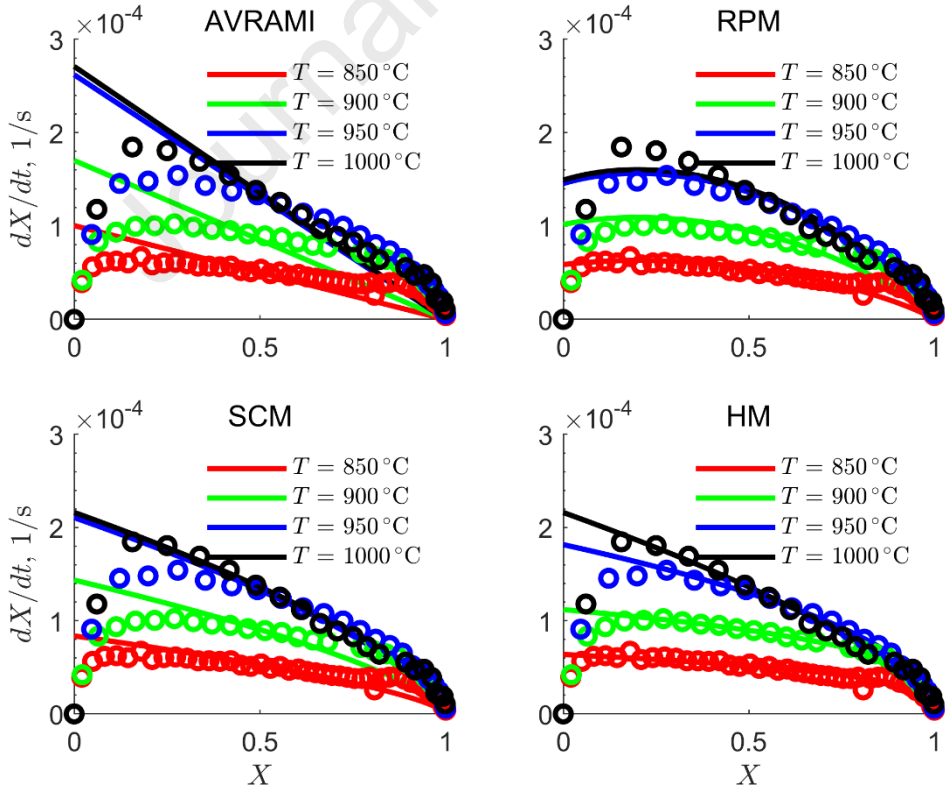

Fig. 17. Comparison of fitted model functions $f(X)$ for reaction with H_2O

In Fig. 18 the $\ln(k)$ vs. $1/T$ plots of the four models are presented, which also show the calculated pre-exponential factor A and activation energy E. In this figure, the data for all temperatures are presented; however, due to the visible reduction in the reaction rate due to diffusion in pores at the highest temperature, the data at 1000 ℃ was excluded from the analysis. Comparing Fig. 13 and Fig. 14 with Fig. 17 and Fig. 18 shows that the reaction rate in O_2 is an order of magnitude greater than that in H_2O. The model parameters were determined and used to verify the predictions by comparing the results with the experimentally-determined conversions, and the comparison is presented in Fig. 19. The model predictions are satisfactory for all the temperatures. As expected, at the highest temperature of 1000 ℃ the reaction rate is limited by reactant diffusion, thus these datapoints were excluded from the analysis and the model parameters were not determined at this temperature. The sums of squared residuals (SSR) were also similar to each other for all models: RPM $SSR = 2.0 \cdot 10^{-7}$, SCM $SSR = 3.6 \cdot 10^{-7}$ and HM $SSR = 3.1 \cdot 10^{-7}$. It was also observed that for the Hybrid Model (HM) the power m (model parameter) changed considerably with temperature. In the results presented in Fig. 17 – Fig. 19, a constant mean value was used. It was therefore verified if the HM model predictions could be improved by introducing a linear dependence on temperature in the m parameter. Indeed, such a modification allowed reduced the sum of squared residuals of the HM model to HM $SSR = 3.1 \cdot 10^{-7}$ and improved the model predictions in the temperature range of the conducted experiments; however, the $m(T)$ function became negative at lower temperatures, which may lead to incorrect predictions at these temperatures and was therefore excluded from this analysis. The determined parameters of all the models are summarised in Table 2, where a recommendation on the best model for reactions with H_2O is also given. Activation energy determined from the thermogravimetric experiments performed by Edreis et al. [14] was

slightly higher, i.e. 165.54 kJ/mol modeled with SCM. However, their experiments were carried out as a temperature program with a low heating rate of 10 K/min, whereas in these tests, the reaction was initiated with the samples already heated up.

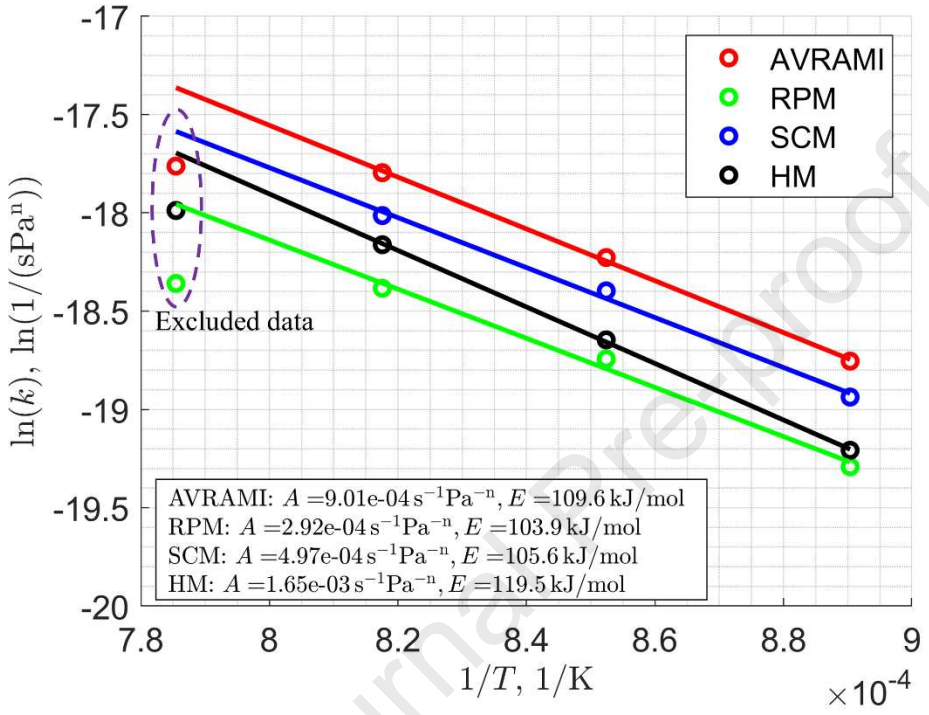

Fig. 18. Determination of the pre-exponential factor A and activation energy E

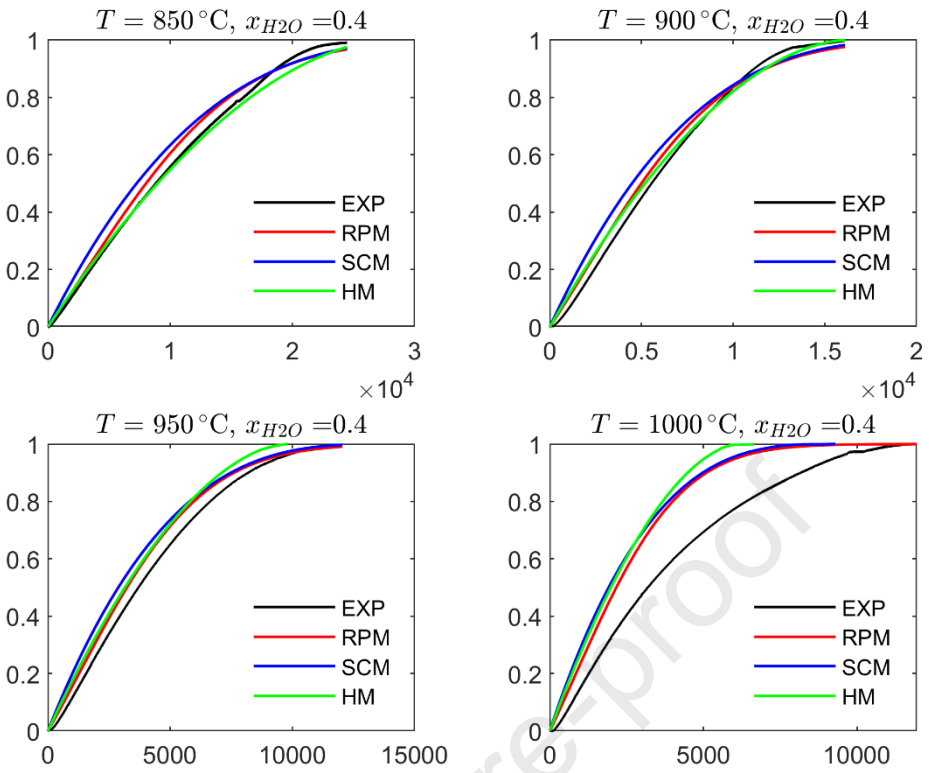

Fig. 19. Comparison of experimental data and model predictions for H_2O/N_2 mixture

Table 2: Summary of the determined model parameters for the reaction of petcoke with H_2O

Model	Equation* $\frac{dX}{dt} = A\exp(-E/RT)f(X)p_{H_2O}^n$	A $1/(\mathrm{sPa}^n)$	E kJ/mol	n	m	ψ
AVRAMI	$f(X) = (1-X)$	9.01e-4	109.57	0.9	-	-
RPM**	$f(X) = (1-X)\sqrt{1-\psi\ln(1-X)}$	**2.92e-4**	**103.91**	**0.9**	**-**	**3.612**
SCM	$f(X) = (1-X)^m$	4.97e-4	105.63	0.9	0.667	-
HM	$f(X) = (1-X)^m$	1.65e-3	119.50	0.9	0.445	-
*p_{H2O} in Pa, T in K; **recommended model						

To further validate the developed models (data from Table 2), they were used to predict conversions vs. time for a set of experimental data obtained for petcoke gasification in H_2O/CO_2 at 900 and 950 ℃ and water vapor mole fractions x_{H2O} of 0.2 and 0.4. Similar to the previous comparison, the AVRAMI model was excluded from the analysis. The comparison is shown in Fig. 20, where the conversions vs. time are presented. The kinetic data obtained for H_2O/N_2 mixtures predicted the experimentally-determined conversions in H_2O/CO_2 mixtures well. Therefore, as stated before, it can be concluded that the role of CO_2 in the process is minor, and, as will be shown in the next section, the reaction with CO_2 in the context of this analysis can be neglected if the temperature does not significantly exceed 1000 ℃.

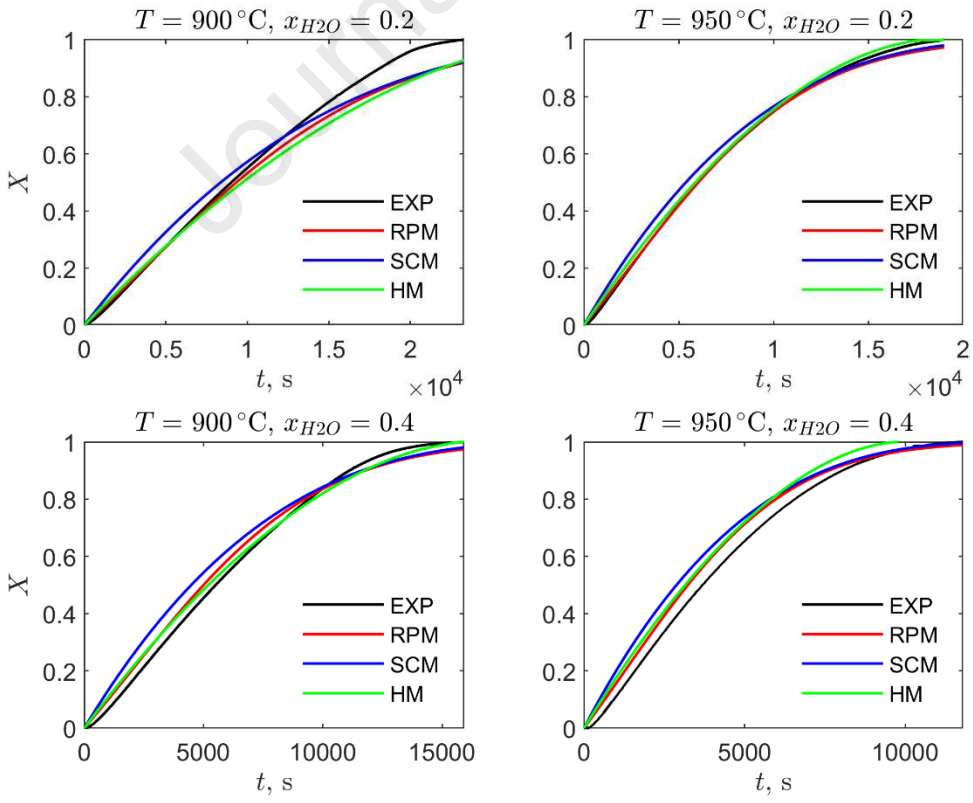

Fig. 20. Comparison of the experimental data for H_2O/CO_2 mixture and model predictions

3.2.3. Reaction with CO_2

The petcoke gasification experiments in a CO_2/N_2 atmosphere ($x_{CO2} = 0.4$ mol/mol) were conducted at three temperatures, i.e. 900, 950, and 1000 ℃. In Fig. 21, the conversion vs. time is presented. The reaction of petcoke with CO_2 is an order of magnitude lower than that with H_2O, and decreases further as the reaction proceeds. It took approximately 6 hours to convert 10 % of the sample at 1000 ℃; thus, the conversion rate is below practical considerations under the analysed conditions. Therefore, no model was proposed here, since for practical systems operating at the temperatures considered in this analysis, the reaction rate can be assumed to be 0. Some literature reports describe the relatively rapid CO_2 gasification of petcoke with activation energies of approximately 150 kJ/mol (e.g. 142 kJ/mol reported by Kumari et al. [16] and 159 kJ/mol reported by Wei et al. [17]). However, those thermogravimetric experiments were performed under the atmosphere of pure CO_2 at temperatures above 1000 ℃, i.e. conditions significantly more reactive than the ones applied in this study.

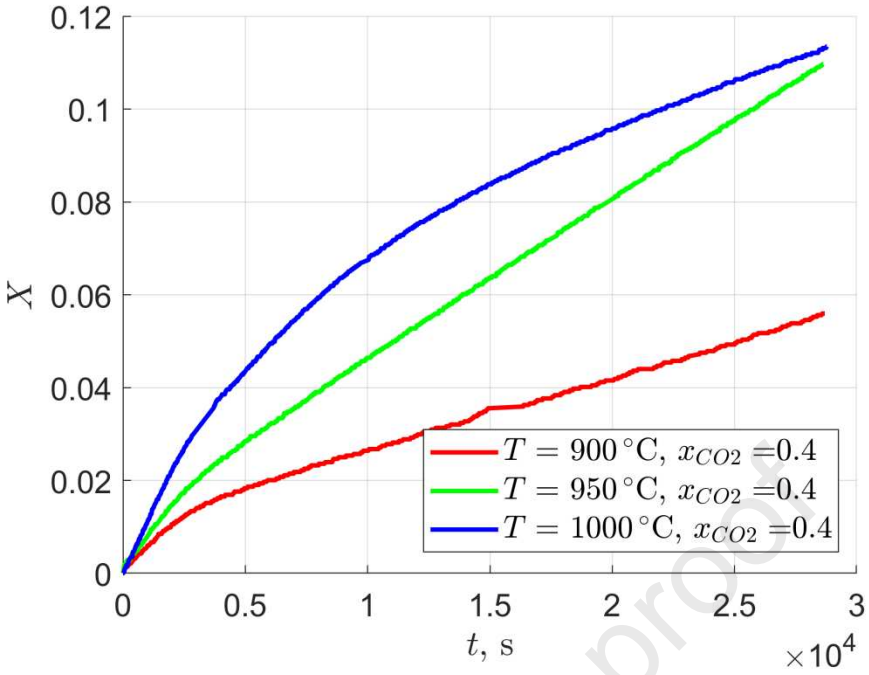

Fig. 21. Conversion vs. time for a reaction with CO_2

4. Conclusions

In this article, the kinetic parameters for petcoke gasification were calculated based on the experimental data from laboratory tests dedicated to the material selected for the CHEERS project, to enable modelling of the 3 MWth prototype of chemical looping combustion (CLC) system with inherent carbon capture.

The tests revealed that the rate of petcoke gasification at 10 and 40 vol.% of CO_2 was negligible at temperatures below 1100 □. The tests allowed the determination of the kinetic parameters for petcoke gasification in steam and oxygen at temperatures up to 950 □. At higher temperatures, the conversion was limited by diffusion. The kinetic parameters of petcoke gasification were best described by:

- the Hybrid Model for gasification in 2-4 % O_2 ($E_a = 15.87$ kJ/mol);

- the Random Pore Model for gasification in 10 – 40 vol.% H_2O ($E_a = 103.91$ kJ/mol).

Moreover, at the temperatures up to 1000 □, conversion in CO_2 was negligible and it did not affect the reaction rate, when CO_2 was added to the steam gasification of petcoke.

The apparent kinetic parameters determined in this work include the internal diffusion within the particles; thus, to make the obtained results more universal, the continuation of this research, to account for different particles sizes, will be considered in the future.

Acknowledgements

This project has received funding from the European Union's Horizon 2020 research and innovation programme under grant agreement No 764697. The project is also co-funded from National Key Research and Development Program of China by Chinese Ministry of Science and Technology (MOST) under grant agreement No 2017YFE0112500.

References

[1] Karasu S, Altan A, Bekiros S, Ahmad W. A new forecasting model with wrapper-based feature selection approach using multi-objective optimization technique for chaotic crude oil time series. Energy 2020;212:118750. https://doi.org/10.1016/j.energy.2020.118750.

[2] Wang J, Anthony EJ, Abanades JC. Clean and efficient use of petroleum coke for combustion and power generation. Fuel 2004;83:1341–8. https://doi.org/10.1016/j.fuel.2004.01.002.

[3] Murthy BN, Sawarkar AN, Deshmukh NA, Mathew T, Joshi JB. Petroleum coke

gasification: A review. Can J Chem Eng 2014;92:441–68. https://doi.org/10.1002/cjce.21908.

[4] Leion H, Mattisson T, Lyngfelt A. The use of petroleum coke as fuel in chemical-looping combustion. Fuel 2007;86:1947–58. https://doi.org/10.1016/j.fuel.2006.11.037.

[5] Lyngfelt A, Linderholm C. Chemical-Looping Combustion of Solid Fuels - Status and Recent Progress. Energy Procedia, vol. 114, Elsevier Ltd; 2017, p. 371–86. https://doi.org/10.1016/j.egypro.2017.03.1179.

[6] Commandré JM, Salvador S. Lack of correlation between the properties of a petroleum coke and its behaviour during combustion. Fuel Process Technol 2005;86:795–808. https://doi.org/10.1016/j.fuproc.2004.08.001.

[7] Tyler RJ. Intrinsic reactivity of petroleum coke to oxygen. Fuel 1986;65:235–40. https://doi.org/10.1016/0016-2361(86)90012-8.

[8] Liu X, Zhou Z, Hu Q, Dai Z, Wang F. Experimental Study on Co-gasification of Coal Liquefaction Residue and Petroleum Coke. Energy & Fuels 2011;25:3377–81. https://doi.org/10.1021/ef200402z.

[9] Wu Y, Wang J, Wu S, Huang S, Gao J. Potassium-catalyzed steam gasification of petroleum coke for H2 production: Reactivity, selectivity and gas release. Fuel Process Technol 2011;92:523–30. https://doi.org/10.1016/j.fuproc.2010.11.007.

[10] Malekshahian M, M. Hill J. Kinetic Analysis of CO2 Gasification of Petroleum Coke at High Pressures. Energy & Fuels 2011;25:4043–8. https://doi.org/10.1021/ef2009259.

[11] Zou JH, Zhou ZJ, Wang FC, Zhang W, Dai ZH, Liu HF, et al. Modeling reaction kinetics of petroleum coke gasification with CO2. Chem Eng Process Process Intensif

2007;46:630–6. https://doi.org/10.1016/j.cep.2006.08.008.

[12] Walsh DE, Green GJ. A laboratory study of petroleum coke combustion: kinetics and catalytic effects. Ind Eng Chem Res 1988;27:1115–20. https://doi.org/10.1021/ie00079a005.

[13] Gajera ZR, Verma K, Tekade SP, Sawarkar AN. Kinetics of co-gasification of rice husk biomass and high sulphur petroleum coke with oxygen as gasifying medium via TGA. Bioresour Technol Reports 2020;11:100479. https://doi.org/10.1016/j.biteb.2020.100479.

[14] Edreis EMA, Li X, Atya AHA, Sharshir SW, Elsheikh AH, Mahmoud NM, et al. Kinetics, thermodynamics and synergistic effects analyses of petroleum coke and biomass wastes during H2O co-gasification. Int J Hydrogen Energy 2020;45:24502–17. https://doi.org/10.1016/j.ijhydene.2020.06.239.

[15] Yu J, Gong Y, Wei J, Ding L, Song X, Yu G. Promoting effect of biomass ash additives on high-temperature gasification of petroleum coke: Reactivity and kinetic analysis. J Energy Inst 2020;93:1364–72. https://doi.org/10.1016/j.joei.2019.12.006.

[16] Kumari N, Saha S, Sahu G, Chauhan V, Roy R, Datta S, et al. Comparison of CO2 gasification reactivity and kinetics: petcoke, biomass and high ash coal. Biomass Convers Biorefinery 2020:1–14. https://doi.org/10.1007/s13399-020-00882-z.

[17] Wei J, Guo Q, Gong Y, Ding L, Yu G. Effect of biomass leachates on structure evolution and reactivity characteristic of petroleum coke gasification. Renew Energy 2020;155:111–20. https://doi.org/10.1016/j.renene.2020.03.132.

[18] Yang H, Song H, Zhao C, Hu J, Li S, Chen H. Catalytic gasification reactivity and mechanism of petroleum coke at high temperature. Fuel 2021;293:120469.

https://doi.org/10.1016/j.fuel.2021.120469.

[19] Wei R, Ren L, Geng F. Gasification reactivity and characteristics of coal chars and petcokes. J Energy Inst 2021;96:25–30. https://doi.org/10.1016/j.joei.2020.07.012.

[20] Wei J, Ding L, Gong Y, Guo Q, Wang Y, Yu G. High□temperature char gasification of anthracite/petroleum coke: using biomass leachate as cheap□effective additive. Asia-Pacific J Chem Eng 2020;15:e2454. https://doi.org/10.1002/apj.2454.

[21] Lulu W, Laihong S, Shouxi J, Tao S. Chemical looping gasification with potassium-catalyzed petroleum coke for enhanced production of H2 and H2S. Chem Eng J 2020;397:124631. https://doi.org/10.1016/j.cej.2020.124631.

[22] Wang Z, Ouyang P, Cui L, Zong B, Wu G, Zhang Y. Valorizing petroleum coke into hydrogen-rich syngas through K-promoted catalytic steam gasification. J Energy Inst 2020;93:2544–9. https://doi.org/10.1016/j.joei.2020.09.001.

[23] Liu L, Li Z, Wu S, Li D, Cai N. Conversion characteristics of lignite and petroleum coke in chemical looping combustion coupled with an annular carbon stripper. Fuel Process Technol 2021;213:106711. https://doi.org/10.1016/j.fuproc.2020.106711.

[24] Zhang J, Hou J, Feng Z, Zeng Q, Song Q, Guan S, et al. Robust modeling, analysis and optimization of entrained flow co-gasification of petcoke with coal using combined array design. Int J Hydrogen Energy 2020;45:294–308. https://doi.org/10.1016/j.ijhydene.2019.10.153.

[25] Fermoso J, Arias B, Pevida C, Plaza M, Rubiera F, Pis J. Kinetic models comparison for steam gasification of different nature fuel chars. J Therm Anal Calorim 2008;91:779–86. https://doi.org/10.1007/s10973-007-8623-5.

[26] Zhan X, Zhou ZJ, Wang F. Catalytic effect of black liquor on the gasification reactivity

of petroleum coke. Appl Energy 2010;87:1710–5. https://doi.org/10.1016/j.apenergy.2009.10.027.

[27] Yoon SJ, Choi Y-C, Lee S-H, Lee J-G. Thermogravimetric study of coal and petroleum coke for co-gasification. Korean J Chem Eng 2007;24:512–7. https://doi.org/10.1007/s11814-007-0090-y.

[28] Ren L, Wei R, Xin J. Co-Gasification Mechanism and Kinetics of Petcoke with Lignite. Energy and Fuels 2020;34:1688–97. https://doi.org/10.1021/acs.energyfuels.9b04144.

[29] Ye DP, Agnew JB, Zhang DK. Gasification of a South Australian low-rank coal with carbon dioxide and steam: kinetics and reactivity studies. Fuel 1998;77:1209–19. https://doi.org/https://doi.org/10.1016/S0016-2361(98)00014-3.

[30] Molina A, Mondragón F. Reactivity of coal gasification with steam and CO2. Fuel 1998;77:1831–9. https://doi.org/https://doi.org/10.1016/S0016-2361(98)00123-9.

[31] Gartner JK, Garcia-Perez M, Van Wie BJ. Investigation of biomass char gasification kinetic parameters using a novel miniaturized educational system. BioResources 2019;14:3594–614. https://doi.org/10.15376/biores.14.2.3594-3614.

[32] Everson RC, Neomagus HWJP, Kaitano R. The random pore model with intraparticle diffusion for the description of combustion of char particles derived from mineral- and inertinite rich coal. Fuel 2011;90:2347–52. https://doi.org/10.1016/j.fuel.2011.03.012.

[33] Trommer D, Noembrini F, Fasciana M, Rodriguez D, Morales A, Romero M, et al. Hydrogen production by steam-gasification of petroleum coke using concentrated solar power - I. Thermodynamic and kinetic analyses. Int J Hydrogen Energy 2005;30:605–18. https://doi.org/10.1016/j.ijhydene.2004.06.002.

[34] Wang J, Jiang M, Yao Y, Zhang Y, Cao J. Steam gasification of coal char catalyzed by K2CO3 for enhanced production of hydrogen without formation of methane. Fuel 2009;88:1572–9. https://doi.org/10.1016/j.fuel.2008.12.017.

[35] Afrooz IE, Ching DLC. A Modified Model for Kinetic Analysis of Petroleum Coke. Int J Chem Eng 2019;2019. https://doi.org/10.1155/2019/2034983.

- Petroleum coke gasification with O_2, CO_2, and H_2O at 750 – 1100 □ was examined
- Evolved gases and sample mass loss were examined in the custom-built test rig
- The interference of external diffusion was avoided at temperatures up to 950 ℃
- Kinetic models were applied to determine kinetic parameters of the gasification

Declaration of interests

☒ The authors declare that they have no known competing financial interests or personal relationships that could have appeared to influence the work reported in this paper.

☐The authors declare the following financial interests/personal relationships which may be considered as potential competing interests: